

# Universality in the dynamics of vesicle translocation through a hole

Bin Zheng,<sup>1,2</sup> Fangfu Ye,<sup>1,2,3,4</sup> Shigeyuki Komura,<sup>1,2,5</sup> and Masao Doi<sup>1,2</sup>

<sup>1</sup>Wenzhou Institute, University of Chinese Academy of Sciences, Wenzhou, Zhejiang 325001, China

<sup>2</sup>Oujiang Laboratory, Wenzhou, Zhejiang 325000, China

<sup>3</sup>School of Physical Science, University of Chinese Academy of Sciences, Beijing 100049, China

<sup>4</sup>Beijing National Laboratory for Condensed Matter Physics,  
Institute of Physics, Chinese Academy of Sciences, Beijing 100190, China

<sup>5</sup>Department of Chemistry, Graduate School of Science,  
Tokyo Metropolitan University, Tokyo 192-0397, Japan

We analyze the translocation process of a spherical vesicle, made of membrane and incompressible fluid, through a hole smaller than the vesicle size, driven by pressure difference  $\Delta P$ . We show that such a vesicle shows certain universal characteristics which is independent of the details of the membrane elasticity; (i) there is a critical pressure  $\Delta P_c$  below which no translocation occurs, (ii)  $\Delta P_c$  decreases to zero as the vesicle radius  $R_0$  approaches the hole radius  $a$ , satisfying the scaling relation  $\Delta P_c \sim (R_0 - a)^{3/2}$ , and (iii) the translocation time  $\tau$  diverges as  $\Delta P$  decreases to  $\Delta P_c$ , satisfying the scaling relation  $\tau \sim (\Delta P - \Delta P_c)^{-1/2}$ .

## I. INTRODUCTION

A vesicle is a fluid droplet covered by a membrane. Examples of natural vesicles are cells and organoids. Artificial vesicles made of amphiphilic copolymers, called polymersomes, have been developed and are used as a capsule of drugs or RNA fragments [1–5]. Translocation of such objects through a constriction is ubiquitous in many biological and bio-technical systems, such as blood flow, cell circulation, drug delivery, and cell manufacturing [6–12].

Many theoretical studies and simulations have been done for vesicle translocation [13–18], but our understanding for these phenomena is still far from complete. One reason is that there exist many types of membranes (lipid membranes, polymer membranes, cell membranes), and it is difficult to construct a general theory valid for all vesicles. Indeed, various models have been used in the past. In the early works [13, 18], it was assumed that the vesicles have constant surface area but have variable volume (as the fluid can permeate through the membrane). In recent works, alternative models have been used in which the vesicle has a constant volume, but has a variable surface area [14, 19, 20]. Another important difference is whether the membrane is a fluid which has zero shear modulus in the plane, or an elastic sheet which has non-zero shear modulus [21]. In most of the previous works, the membrane has been assumed to be a fluid membrane, but an elastic membrane, often called the tethered membrane, exists and is important in many biological systems. Translocation of such membranes has been studied recently by computer simulations [15].

In this work, we develop a theory for vesicle translocation using a model which can include a large class of membranes such as fluid membranes, tethered membranes, and composite membranes. The model assumes that (i) the elastic energy of the membrane is due to the in-plane stretching of the membrane (i.e., the bending energy of the membrane is ignorable), (ii) the volume

of the vesicle is kept constant during translocation (i.e., the fluid permeation through the membrane is ignorable), and (iii) the vesicle takes a spherical shape outside of the hole. We show that if a vesicle satisfies these conditions, its translocation behavior has certain universal characteristics which are independent of the details of the membrane property.

The outline of the article is as follows. In Sec. II, we discuss the general form of the free energy of a stretchable membrane model, and give two specific models: (i) fluid membrane model and (ii) rubber membrane model. Time-evolution equation for the vesicle during translocation is derived. In Sec. III, we show the free energy profile for the translocation process, and calculate the critical pressure needed to cause the translocation. We then show that there is certain universality in the critical pressure and the translocation time. Finally, in Sec. IV, we summarize our result and compare it with previous simulation works.

## II. THEORY

### A. General membrane model

We consider a spherical vesicle consisting of membrane and inner fluid. The membrane can be a single layer of amphiphilic molecules (uncross-linked or cross-linked polymers as in polymersomes) or composite membranes made of a fluid layer and elastic networks (as in plasma membranes).

We regard the membrane as a 2D surface, described by a 3D position vector  $\mathbf{r}(s_1, s_2)$ , where  $s_1$  and  $s_2$  are the 2D coordinates which are defined in the reference state and identify a point in the membrane. We assume that, in the reference state,  $\partial\mathbf{r}/\partial s_1$  and  $\partial\mathbf{r}/\partial s_2$  are unit vectors orthogonal to each other. (When we use the spherical coordinate  $(\theta, \psi)$ ,  $s_1$  and  $s_2$  can be written as  $s_1 = R^*\theta$  and  $s_2 = (R^*\sin\theta)\psi$ , where  $R^*$  is the ra-

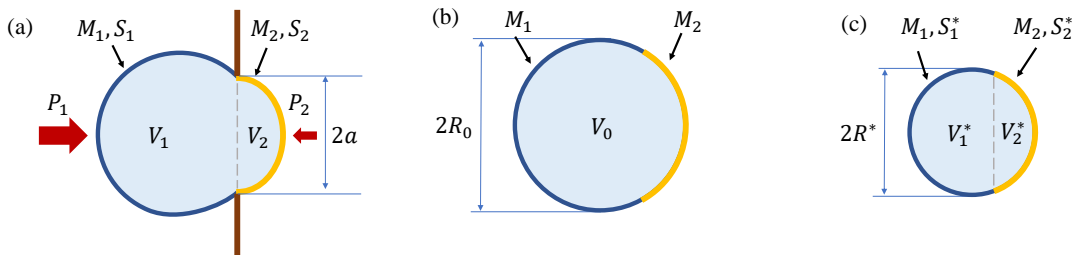


FIG. 1. (a) When a vesicle is translocating through a hole of radius  $a$ , it takes a double-spherical cap shape. The volume of the vesicle in each chamber is  $V_1$  and  $V_2$ , and the area and the mass of the membrane in each chamber are  $S_i$  and  $M_i$  ( $i = 1, 2$ ), respectively. (b) Outside of the hole, the vesicle takes a spherical shape of volume  $V_0 = V_1 + V_2$ . The parts of the membrane which are in chamber 1 or 2 in the state (a) are shown by different colors. (c) The vesicle in the reference state where the vesicle takes a spherical shape of radius  $R^*$ . The stretching  $\lambda_i$  of the membrane is defined by the length change with respect to this state. Notice that the volume  $V_0$  in the state (b) is generally different from the volume  $V^* = V_1^* + V_2^*$  in the state (c).

dius of the sphere.) We assume that the membrane is homogeneous and isotropic in the tangential plane. We also assume that the membrane is thin and ignore the bending energy. The elastic energy of the membrane is therefore due to the in-plane membrane stretching and can be characterized by the function  $f(\lambda_1, \lambda_2)$ , where  $\lambda_1$  and  $\lambda_2$  are the principal values of stretching and  $f(\lambda_1, \lambda_2)$  is the elastic energy per unit area in the reference state. ( $\lambda_1$  and  $\lambda_2$  are given by the square root of the eigenvalues of the  $2 \times 2$  matrix  $B_{ij} = (\partial \mathbf{r} / \partial s_i) \cdot (\partial \mathbf{r} / \partial s_j)$  with  $i, j = 1, 2$ .) The total elastic energy functional of the membrane is given by the integral of  $f(\lambda_1, \lambda_2)$  over the entire surface:

$$\mathcal{A}[\mathbf{r}(s_1, s_2)] = \int ds_1 ds_2 f(\lambda_1, \lambda_2). \quad (1)$$

The equilibrium state of the membrane is calculated by minimizing this functional with respect to  $\mathbf{r}(s_1, s_2)$ .

For fluid membranes,  $f(\lambda_1, \lambda_2)$  depends only on the area change ratio  $\lambda_1 \lambda_2$ . In this work, we consider the following model energy

$$f_{\text{FM}}(\lambda_1, \lambda_2) = \frac{k_a}{2} (\lambda_1 \lambda_2 - 1)^2, \quad (2)$$

where  $k_a$  is the elastic constant, which has the same dimension as the surface tension.

For elastic (or tethered) membranes,  $f$  cannot be written in this form because they experience restoring force caused by shear strain  $\lambda_1 - \lambda_2$ . As an example, we consider the following Neo-Hookean model [22], which has been extensively used as a model of rubber membrane (such as balloons)

$$f_{\text{RM}}(\lambda_1, \lambda_2) = \frac{\mu d}{2} [\lambda_1^2 + \lambda_2^2 + (\lambda_1 \lambda_2)^{-2} - 3], \quad (3)$$

where  $\mu$  is the 3D shear modulus of the rubber and  $d$  is the thickness of the membrane. We call such a membrane a rubber membrane.

## B. Free energy of a vesicle under translocation

We now consider the situation that such a vesicle is forced to pass through a hole of radius  $a$  made in a wall at the boundary between two chambers 1 and 2, as shown in Fig. 1. Initially, the vesicle has a spherical shape of radius  $R^*$  [Fig. 1(c)] and it is inflated to have a radius  $R_0$  by some methods (e.g., osmotic swelling or injection) [Fig. 1(b)]. We use the swelling ratio defined by  $\eta = R_0/R^* \geq 1$ . The pressure in each chamber is  $P_1$  and  $P_2$ , and the vesicle is pushed by the pressure difference  $\Delta P = P_1 - P_2 > 0$ . During the translocation, the vesicle takes a double spherical-cap shape, each having volume  $V_1$  and  $V_2$  [Fig. 1(a)]. Since the membrane is assumed to be impermeable to the fluid during the passage, the total fluid volume  $V_0 = V_1 + V_2 = 4\pi R_0^3/3$  remains unchanged. Let  $S_1$  and  $S_2$  be the area of the membrane in each chamber. Since the membrane can be stretched, the total area of the membrane  $S = S_1 + S_2$  can vary. To describe the transport of the membrane, we introduce the membrane mass  $M_1$  and  $M_2$  in each chamber. The total mass  $M_0 = M_1 + M_2$  remains constant, but the membrane mass density  $M_i/S_i$  ( $i = 1, 2$ ) in each chamber changes in time.

Given the free energy functional such as Eq. (1), the free energy of the vesicle is uniquely determined as a function of  $M_i$  and  $V_i$ , and is written as

$$G = A(M_1, V_1) + A(M_2, V_2) + P_1 V_1 + P_2 V_2, \quad (4)$$

where  $A(M_i, V_i)$  is the minimum of the functional  $\mathcal{A}[\mathbf{r}(s_1, s_2)]$  subject to the constraint that the membrane has mass  $M_i$  and includes fluid volume  $V_i$ , and that its circular edge is fixed to the hole of radius  $a$ . In the following, we calculate  $A(M_i, V_i)$  explicitly for a fluid membrane and a rubber membrane.

### 1. Fluid membrane

We first consider the fluid membrane model. The fluid membrane at equilibrium always takes a spherical-cap

shape with constant curvature. Therefore the integral of Eq. (2) can be written as  $S_i^* f(S_i/S_i^*)$ , and the total free energy can be written as

$$G(M_i, V_i) = \frac{k_a}{2} \frac{[S_1(V_1) - S_1^*(M_1)]^2}{S_1^*(M_1)} + \frac{k_a}{2} \frac{[S_2(V_2) - S_2^*(M_2)]^2}{S_2^*(M_2)} + P_1 V_1 + P_2 V_2, \quad (5)$$

where  $S_i^* = 4\pi(R^*)^2 M_i/M_0$  is the area of the membrane of mass  $M_i$  in the reference state [Fig. 1(c)]. The surface area  $S_i$  is determined by the condition that the spherical cap has volume  $V_i$  and its edge is fixed to a circle of radius  $a$ . This condition leads to  $S_i = \pi(a^2 + h_i^2)$ , where  $h_i$  is the solution of the equation  $V_i = \pi h_i(3a^2 + h_i^2)/6$  for given  $V_i$ . Therefore, the energy of the fluid membrane can be expressed in terms of  $M_i$  and  $V_i$ .

Since  $V_0 = V_1 + V_2$  and  $M_0 = M_1 + M_2$  are constant, the total free energy  $G$  can be expressed as a function of  $V_2$  and  $M_2$ . We define the following dimensionless quantities

$$x = \frac{M_2}{M_0} - \frac{1}{2}, \quad y = \frac{V_2}{V_0} - \frac{1}{2}, \quad (6)$$

and write the total free energy as

$$G(x, y) = \frac{k_a}{2} \frac{[S_1(y) - (1/2 - x)S^*]^2}{(1/2 - x)S^*} + \frac{k_a}{2} \frac{[S_2(y) - (1/2 + x)S^*]^2}{(1/2 + x)S^*} - \Delta P V_0 y, \quad (7)$$

where  $S^* = S_0/\eta^2$  and  $\eta = R_0/R^*$  is the swelling ratio. In addition,  $S_2/S_0$  can be derived from the geometric relation for a spherical cap as mentioned above, and becomes

$$\frac{S_2(y, a/R_0)}{S_0} = -\frac{(a/R_0)^2}{4} + \frac{(a/R_0)^4}{4\beta^{2/3}} + \frac{\beta^{2/3}}{4}, \quad (8)$$

where

$$\beta(y, a/R_0) = 4(y + 1/2) + \sqrt{(a/R_0)^6 + 16(y + 1/2)^2}. \quad (9)$$

Similarly,  $S_1(y, a/R_0)/S_0$  is obtained by replacing  $y$  with  $-y$  in the above equation.

## 2. Rubber membrane

We next consider the rubber membrane whose free energy is given by Eq. (3). To calculate the elastic free energy, we first focus on the spherical cap in chamber 2, which has the surface mass  $M_2$  and is initially a part of the equilibrium vesicle of radius  $R^*$ . Then, it is fixed to the hole of radius  $a$  and is inflated to the volume  $V_2$  as shown by the yellow curve in Fig. 1(a).

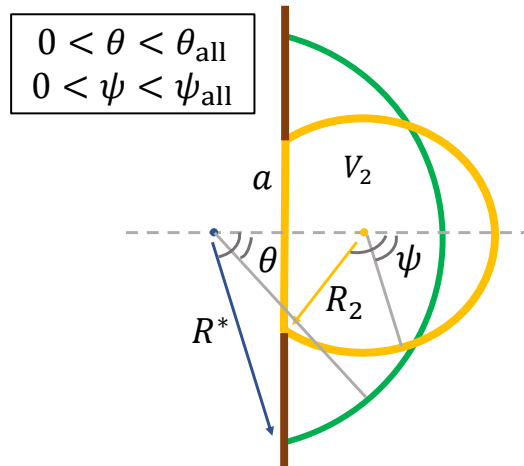


FIG. 2. Schematic illustration of the rubber membrane model.

Exact calculation of the elastic energy for such deformation is difficult for a rubber membrane. Here we use an approximation and assume that the membrane takes a spherical shape of curvature  $1/R_2$ , as shown in Fig. 2. Then, a point located at a polar angle  $\theta$  on the sphere of radius  $R^*$  in the reference state will move to a point located at a polar angle  $\psi(\theta)$  on the inflated sphere of radius  $R_2$ . This deformation elongates the line segment along the  $\theta$  direction by factor  $R_2 d\psi/R^* d\theta$ , and the line segment perpendicular to this direction by factor  $R_2 \sin \psi/R^* \sin \theta$ . Hence the principal values of stretching in chamber 2 are given by

$$\lambda_{21} = \frac{R_2}{R^*} \frac{d\psi}{d\theta}, \quad \lambda_{22} = \frac{R_2 \sin \psi}{R^* \sin \theta}. \quad (10)$$

To determine the functional form of  $\psi(\theta)$ , we assume that the surface area of the membrane changes uniformly by deformation, such that  $\lambda_{21}\lambda_{22}$  is constant (independent of  $\theta$ ). This condition gives

$$\frac{\sin \psi}{\sin \theta} \frac{d\psi}{d\theta} = \text{Const.} \quad (11)$$

From this relation, we have

$$\frac{1 - \cos \theta}{1 - \cos \psi} = \frac{1 - \cos \theta_{\text{all}}}{1 - \cos \psi_{\text{all}}}, \quad (12)$$

where  $\theta_{\text{all}}$  and  $\psi_{\text{all}}$  are the maximum values of  $\theta$  and  $\psi$ , respectively, which are given by (see Fig. 2)

$$\theta_{\text{all}} = \arccos(-2x), \quad (13)$$

$$\psi_{\text{all}} = \arccos \left[ 1 - \frac{2S_2/S_0}{(R_2/R_0)^2} \right]. \quad (14)$$

Here,  $R_2(y)/R_0$  can be derived from the geometric relation for a spherical cap,  $S_2 = 2\pi R_2 h_2$ , where  $h_2$  is the solution of the equation  $V_2 = \pi h_2^2(3R_2 - h_2)/3$ . On the

other hand,  $S_2(y, a/R_0)/S_0$  is given by Eqs. (8) and (9). Then, the same calculation can be done for the membrane in chamber 1.

The total energy of deformation can be expressed by the integrals over  $\theta$

$$G(x, y) = \frac{\mu d}{2} \int_0^{\pi - \theta_{\text{all}}} d\theta \left( \lambda_{11}^2 + \lambda_{12}^2 + \frac{1}{\lambda_{11}^2 \lambda_{12}^2} - 3 \right) \times 2\pi (R^*)^2 \sin \theta + \frac{\mu d}{2} \int_0^{\theta_{\text{all}}} d\theta \left( \lambda_{21}^2 + \lambda_{22}^2 + \frac{1}{\lambda_{21}^2 \lambda_{22}^2} - 3 \right) \times 2\pi (R^*)^2 \sin \theta - \Delta P V_0 y. \quad (15)$$

Although, the above integrals can be performed analytically, it is too lengthy to present the result here.

### C. Time-evolution equation

If the free energy of the system is expressed as a function of  $x$  and  $y$ , their time evolution can be discussed in the same way as in the previous works [20]. Here, it is important to note that the characteristic times of  $x$  and  $y$  are quite different from each other. The membrane mass transport is governed by the solid friction of the membrane sliding against the hole, while the fluid volume transport is governed by the fluid flow through the hole. Since the fluid friction is much smaller than the solid friction, the relaxation time of  $y$  is much smaller than that of  $x$ . Therefore we may assume that  $y$  is at equilibrium for a given value of  $x$ . Hence,  $y$  is determined by the condition

$$\frac{\partial G(x, y)}{\partial y} = 0. \quad (16)$$

Let  $y = y^*(x)$  be the solution of this equation. The total free energy is therefore written as a function of  $x$  only and we write it as

$$G_x^* = G(x, y^*(x)). \quad (17)$$

Then the time-evolution equation for  $x$  is written as

$$\xi(x) \frac{dx}{dt} = -\frac{dG_x^*}{dx}, \quad (18)$$

where  $\xi(x)$  is the friction coefficient representing the solid friction for the membrane sliding at the hole rim.

## III. RESULTS

### A. Free energy profile

Figure 3 shows an example of  $G_x^*$  calculated for a fluid membrane whose free energy is given by Eq. (7). When there is no pressure difference, i.e., when  $\Delta P = 0$ ,  $G_x^*$  has

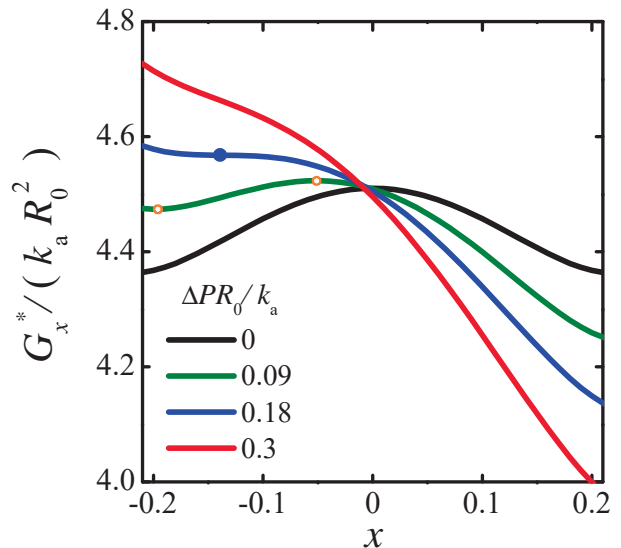


FIG. 3. The free energy  $G_x^*$  of a fluid membrane as a function of  $x = M_2/M_0 - 1/2$  when  $a/R_0 = 0.9$  for different values of  $\Delta P$ .

a peak at  $x = 0$ . When a small pressure is applied,  $G_x^*$  has a local minimum in the region of  $x < 0$ . This corresponds to the situation that the vesicle is trapped by the hole. By the further increase of  $\Delta P$ , the local minimum becomes unstable (see the curve of  $\Delta P R_0 / k_a \approx 0.18$  in Fig. 3). The vesicle translocates from chamber 1 to 2 above this critical pressure difference.

### B. Critical pressure for translocation

The above argument shows that the critical pressure difference  $\Delta P_c$  is determined by the following condition for general membranes

$$\frac{dG_x^*}{dx} = \frac{d^2 G_x^*}{dx^2} = 0. \quad (19)$$

Although  $\Delta P_c$  can be obtained by solving Eq. (19), the calculation becomes somewhat cumbersome. However, there is a simpler way of calculating  $\Delta P_c$ .

We consider the function  $G_y^* = G(x^*(y), y)$ , where  $x^*(y)$  is the solution of  $\partial G(x, y) / \partial x = 0$ . In Appendix A, we show that the critical state can also be obtained by solving the following equations:

$$\frac{dG_y^*}{dy} = \frac{d^2 G_y^*}{dy^2} = 0. \quad (20)$$

The advantage of using  $G_y^*$  is that  $x^*(y)$  is independent of  $\Delta P$  and satisfies the symmetry relation  $x^*(-y) = -x^*(y)$ . Hence,  $G_y^*$  can be written in the following form:

$$G_y^* = A_{\text{tot}}(y) - \Delta P V_0 y, \quad (21)$$

where  $A_{\text{tot}}(y)$  stands for the minimum of the total membrane elastic energy [i.e.,  $A_{\text{tot}}(y) = \text{Min}(A(M_1, V_1) +$

$A(M_2, V_2)$ ] subject to the constraint that the inner fluid volume in chamber 2 is  $(1/2 + y)V_0$ . Notice that  $A_{\text{tot}}(y)$  satisfies the relation  $A_{\text{tot}}(-y) = A_{\text{tot}}(y)$ .

Further simplification is possible for fluid membranes for which  $A(M_i, V_i)$  can be written as  $S_i^* f(S_i/S_i^*)$ . Then the condition  $\partial G(x, y)/\partial x = 0$  gives the relation  $S_1/S_1^* = S_2/S_2^* = S/S^*$ , where  $S = S_1 + S_2$  is the total surface area of the vesicle and  $S^* = S_0/\eta^2$ . The free energy  $G_y^*$  can be written as

$$\begin{aligned} G_y^* &= S_1^* f(S_1/S_1^*) + S_2^* f(S_2/S_2^*) - \Delta P V_0 y \\ &= S^* f(S/S^*) - \Delta P V_0 y. \end{aligned} \quad (22)$$

For given  $a$  and  $R_0$ ,  $S$  depends only on  $y$ . For Eq. (22), the first equation in Eq. (20) gives the following equilibrium pressure  $\Delta P$  at state  $y$ ,

$$\Delta P = \frac{f'}{V_0} \frac{dS}{dy}. \quad (23)$$

The second equation in Eq. (20) gives the following equation for  $y_c$  at the critical state

$$\frac{f''}{S^*} \left( \frac{dS}{dy} \right)^2 + f' \frac{d^2 S}{dy^2} = 0, \quad (24)$$

where  $f'$  and  $f''$  stand for the first and the second derivatives of the function  $f$ , respectively. In addition,  $S/S_0$  is derived from the geometric relation for a spherical cap and is given by Eqs. (8) and (9). Finally, the analytical expression of  $\Delta P$  in Eq. (23) can be obtained, but it is too lengthy to present it here.

In Fig. 4(a), we plot  $\Delta P_c$  of the fluid membrane described by Eq. (2) when  $\eta = R_0/R^* = 1.5$ . Naturally,  $\Delta P_c$  approaches to zero for  $a/R_0 \rightarrow 1$ . In Fig. 4(b), we show the dependence of  $\Delta P_c$  on  $1 - a/R_0$  in the double logarithmic plot. The plot indicates the scaling relation  $\Delta P_c \sim (1 - a/R_0)^\alpha$ . The exponent is  $\alpha = 3/2$  for most cases, whereas the only exception is the case of  $\eta = 1$  (unswollen vesicle) for which we have  $\alpha = 7/2$ .

Further analytical calculation of  $\Delta P_c$  is possible when  $\varepsilon_a = 1 - a/R_0$  is small. For  $\varepsilon_a \ll 1$ , we obtain

$$\Delta P_c \approx \frac{16\sqrt{6}}{9} \frac{k_a}{R_0} \frac{[(\eta^2 - 1)\varepsilon_a + (10 - 7\eta^2)\varepsilon_a^3/3]^{3/2}}{[(\eta^2 - 1) + 3(5 - 4\eta^2)\varepsilon_a^2]^{1/2}}. \quad (25)$$

This expression explicitly shows that, apart from the special case of  $\eta = 1$ , the exponent is  $\alpha = 3/2$ . In the limit of  $\eta \gg 1$ , the critical pressure becomes

$$\Delta P_c \approx \frac{16\sqrt{6}}{9} \frac{\gamma}{R_0} \varepsilon_a^{3/2}, \quad (26)$$

where  $\gamma = \eta^2 k_a$  is the effective surface tension of the vesicle at the initial state. In the limit of  $\eta \gg 1$ , the area change of the vesicle during translocation is small, and the vesicle can be regarded as a liquid droplet (without any membrane) having the constant surface tension  $\gamma$  [23]. Indeed, the same result can be obtained from the analysis of a liquid droplet whose shape is controlled only by surface tension, as shown in Appendix B.

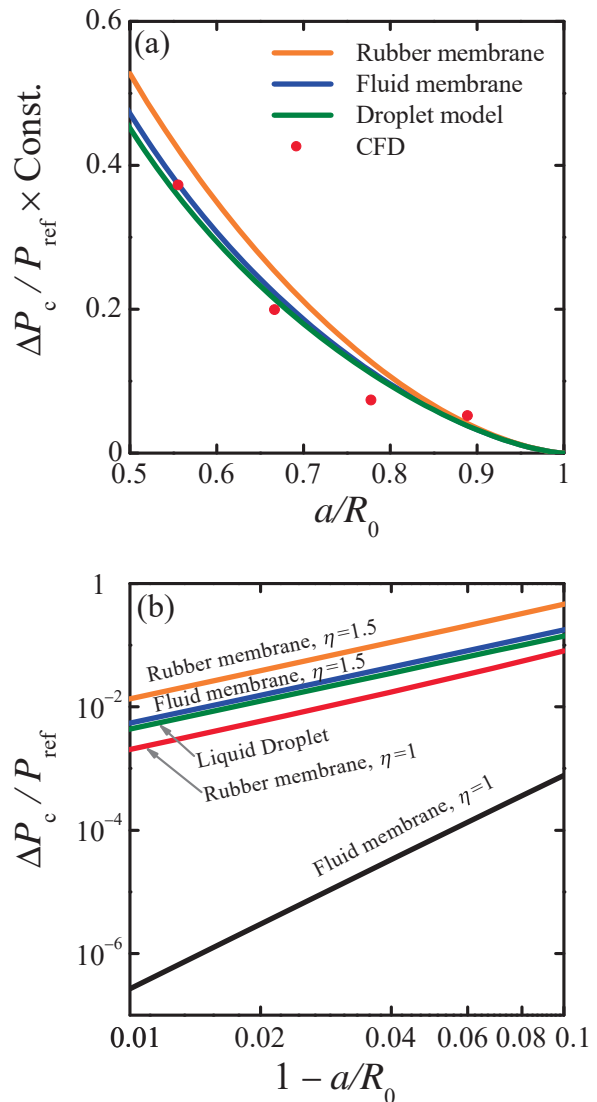


FIG. 4. (a) The reduced critical pressure  $\Delta P_c/P_{\text{ref}}$  as a function of  $a/R_0$  for different membrane models when  $\eta = R_0/R^* = 1.5$ . Here,  $P_{\text{ref}}$  corresponds to  $k_a/R_0$  for a fluid membrane,  $\mu d/R_0$  for a rubber membrane, and  $\gamma/R_0$  for a liquid droplet, respectively. The constant factors in  $\Delta P_c/P_{\text{ref}}$  are chosen to have an overlap of different curves when  $a/R_0$  is close to unity. The red circles are the data obtained by the computational fluid dynamics (CFD) in Ref. [10]. (b) The double logarithmic plot of (a) as a function of  $1 - a/R_0$  for different membrane models when  $\eta = 1.5$  and 1.

### C. Universality in the critical pressure

We have shown that the critical pressure approaches zero as the hole size approaches the equilibrium vesicle size according to the scaling relation  $\Delta P_c \propto (1 - a/R_0)^{3/2}$ . We now show that, apart from the exceptional case, the exponent  $\alpha = 3/2$  is always valid for spherical vesicles (for both fluid and elastic membranes) as long as the free energy is written in the form of Eq. (4).

We start from the expression for the free energy in Eq. (21) that is valid for  $|y|$  less than a certain value  $y_m > 0$ . This range of  $y$  gets smaller as  $\varepsilon_a$  gets smaller. Therefore we may expand  $A_{\text{tot}}(y)$  with respect to  $y$ . Since  $A_{\text{tot}}(y)$  is an even function of  $y$ ,  $G_y^*$  can be written as

$$G_y^* \approx -\Delta P V_0 y - B_1 y^2 + B_2 y^4 + \dots, \quad (27)$$

The coefficients  $B_1$  and  $B_2$  depend on the vesicle properties (e.g., size and elasticity) and also on the hole size  $a$ . For small  $\Delta P > 0$ ,  $G_y^*$  has a local minimum at a certain value of  $y$  that satisfies  $-y_m < y < 0$ . As  $\Delta P$  increases, the local minimum disappears and  $G_y^*$  becomes a monotonically decreasing function of  $y$ . For  $G_y^*$  to have such a shape change, both  $B_1$  and  $B_2$  must be positive, whereas the coefficient  $B_1$  has to vanish as  $\varepsilon_a \rightarrow 0$ . Hence we may assume  $B_1 = b_1 \varepsilon_a$  where  $b_1$  is a positive constant. Then Eqs. (20) and (27) give the following critical state

$$y_c = -\left(\frac{b_1 \varepsilon_a}{6B_2}\right)^{1/2}, \quad \Delta P_c = \frac{2\sqrt{6}b_1^{3/2}\varepsilon_a^{3/2}}{9V_0 B_2^{1/2}}. \quad (28)$$

The latter result shows that the relation  $\Delta P_c \sim \varepsilon_a^{3/2}$  holds generally and is independent of the detail of the membrane property.

The singular behavior for a fluid membrane when  $\eta = 1$  (black line in Fig. 4(b)) arises from the fact that  $b_1$  in the above argument vanishes. If the vesicle is swollen ( $\eta > 1$ ) or if the membrane is tethered,  $b_1$  becomes nonzero and the exponent  $\alpha = 3/2$  is recovered. To demonstrate this, we calculate  $\Delta P_c$  for a rubber membrane with Eq. (15) and the result is shown in Fig. 4 (b). For the rubber membrane, we see that the exponent  $\alpha$  does not show any singularity at  $\eta = 1$ , as shown by the orange and red lines in Fig. 4(b).

#### D. Universality in the translocation time

Finally, we consider the vesicle translocation time  $\tau$ , i.e., the time needed for the vesicle to pass through the hole. It can be calculated by integrating  $(dx/dt)^{-1}$  in Eq. (18) from the initial value to the final value:

$$\tau = \int_{-x_m}^{x_m} dx \xi(x) \left(-\frac{dG_x^*}{dx}\right)^{-1}, \quad (29)$$

where  $x_m$  defines the range of the integration. The translocation time  $\tau$  diverges as  $\Delta P$  approaches to  $\Delta P_c$ . The relation between  $\tau$  and  $\Delta P - \Delta P_c$  can be obtained by the similar phenomenological argument as before.

We consider the situation that  $\Delta P$  is slightly larger than  $\Delta P_c$ . We define a dimensionless parameter  $\varepsilon_P = \Delta P/\Delta P_c - 1 > 0$ , which is small in the current situation. Then, the translocation time is essentially determined by the time needed for the vesicle to pass through the small region near the critical point  $x_c$ . In such a case,

the friction coefficient  $\xi(x)$  can be replaced by a constant  $\xi_c = \xi(x_c)$  and the derivative of  $G_x^*$  can be expanded in terms of  $x - x_c$  as

$$-\frac{dG_x^*}{dx} = C_0 + C_1(x - x_c) + C_2(x - x_c)^2 + \dots, \quad (30)$$

where the coefficients  $C_i$  ( $i = 0, 1, 2, \dots$ ) are functions of  $\varepsilon_P$ . The condition for the critical state in Eq. (19) imposes that  $C_0$  and  $C_1$  must vanish when  $\varepsilon_P = 0$ . We may thus assume  $C_0 = c_0 \varepsilon_P$  and  $C_1 = c_1 \varepsilon_P$ . In the limit of  $\varepsilon_P \rightarrow 0$ , the integral becomes independent of  $x_m$  and  $c_1$ , and approaches to the following asymptotic value:

$$\tau \approx \int_{-\infty}^{\infty} dx \frac{\xi_c}{c_0 \varepsilon_P + C_2(x - x_c)^2} = \frac{\pi \xi_c \varepsilon_P^{-1/2}}{(c_0 C_2)^{1/2}}. \quad (31)$$

Therefore, the translocation time is proportional to  $(\Delta P - \Delta P_c)^{-1/2}$ , which is another universal property of the vesicle translocation.

## IV. SUMMARY AND DISCUSSION

In summary, we have shown that there is a universality in the translocation of a wide class of vesicles which take spherical shapes in the free state: (i) there is a critical pressure difference  $\Delta P_c$  for the translocation to take place, (ii) the critical pressure obeys the scaling relation  $\Delta P_c \sim (R_0 - a)^{3/2}$ , and (iii) the translocation time diverges as  $\tau \sim (\Delta P - \Delta P_c)^{-1/2}$ . We have shown that they are in agreement with rigorous calculations for fluid membranes and an approximate calculation for rubber membranes.

So far, there are scarce data (experimental or simulation) to be compared with our predictions. The critical pressure for a droplet passing through a channel was studied by numerically solving the hydrodynamic equations [10], and they are plotted by the red circles in Fig. 4(a). Furthermore, we give a simple estimation of  $\Delta P_c$  by using Eq. (25). In the experiment, the typical radius of a polymersome is  $R_0 \approx 20 \mu\text{m}$  and its stretching modulus is  $k_a \approx 0.1 \text{ N/m}$  [3]. Considering  $a/R_0 = 0.8$  and  $\eta = 2$ , we obtain  $\Delta P_c \approx 3 \times 10^3 \text{ Pa}$  which is consistent with the above work [10].

Other work to be compared is the molecular dynamics simulation for the translocation of tethered vesicles by Rangelov *et al.* [15]. They reported the existence of  $\Delta P_c$ , and studied the exponent  $\omega$  which describes the divergence of the translocation time as  $\tau \sim (\Delta P - \Delta P_c)^{-\omega}$ . They found that  $\omega$  varies from 0.22 to 0.85 depending on the hole size. Although our theory is not in contradiction with their results, the reason for the deviation needs to be studied. More studies are needed to confirm the validity of the present theory.

## ACKNOWLEDGMENTS

B.Z., S.K., and M.D. acknowledge the startup fund of Wenzhou Institute, University of Chinese Academy of Sciences (Nos. WIUCASQD2022016, WIUCASQD2021041, and WIUCASQD2022004) and Oujian Laboratory (No. OJQDSP2022018). B.Z. and S.K. acknowledge the National Natural Science Foundation of China (NSFC) through Grants (Nos. 22203022, 12274098, and 12250710127).

### Appendix A: Proof of equivalence of the two ways in determining critical points

We consider a free energy function  $G(x, y, P)$  which has two independent variables  $x$  and  $y$  and include a parameter  $P$ . The equilibrium state is given by

$$\frac{\partial G}{\partial x} = 0, \quad \frac{\partial G}{\partial y} = 0. \quad (\text{A1})$$

Suppose that the above local minimum becomes unstable at a certain critical value  $P_c$ . It can be obtained in two ways.

- (i)  $P_c$  is obtained by solving the following set of equations

$$\begin{aligned} \frac{\partial G}{\partial x} = 0, \quad \frac{\partial G}{\partial y} = 0, \\ \frac{\partial^2 G}{\partial x^2} \frac{\partial^2 G}{\partial y^2} - \left( \frac{\partial^2 G}{\partial x \partial y} \right)^2 = 0. \end{aligned} \quad (\text{A2})$$

The first two equations indicate that  $G(x, y)$  becomes stationary at  $(x_c, y_c)$ , and the third equation indicates that the same stationary state is at the stability limit.

- (ii) We reduce the two variables function  $G(x, y)$  to a one-variable function

$$G_x^* = \min_y G(x, y) = G(x, y^*(x)), \quad (\text{A3})$$

where  $y^*(x)$  is the solution of  $\partial G/\partial y = 0$ . Then  $P_c$  is obtained by the condition that the local minimum of  $G_x^*$  becomes unstable at  $P_c$ :

$$\frac{dG_x^*}{dx} = 0, \quad \frac{d^2G_x^*}{dx^2} = 0. \quad (\text{A4})$$

These two methods are equivalent and give the same value for  $P_c$ . This is proven as follows.

We use the formula:

$$\frac{dG(x, y^*(x))}{dx} = \frac{\partial G}{\partial x} + \frac{\partial G}{\partial y} \frac{dy^*}{dx}. \quad (\text{A5})$$

Then using the relation  $\partial G(x, y^*)/\partial y = 0$ , we obtain

$$\frac{dG_x^*}{dx} = \frac{\partial G}{\partial x} + \frac{\partial G}{\partial y} \frac{dy^*}{dx} = \frac{\partial G(x, y^*)}{\partial x}. \quad (\text{A6})$$

By using Eq. (A5), we have

$$\frac{d^2G_x^*}{dx^2} = \frac{\partial^2 G}{\partial x^2} + \frac{\partial^2 G}{\partial x \partial y} \frac{dy^*}{dx}. \quad (\text{A7})$$

On the other hand, since  $\partial G(x, y^*)/\partial y = 0$ , we have

$$\frac{d}{dx} \left( \frac{\partial G(x, y^*)}{\partial y} \right) = \frac{\partial^2 G}{\partial y \partial x} + \frac{\partial^2 G}{\partial y^2} \frac{dy^*}{dx} = 0. \quad (\text{A8})$$

Therefore,  $dy^*/dx = -(\partial^2 G/\partial x \partial y)/(\partial^2 G/\partial y^2)$ . Hence the second condition in Eq. (A4) is written as

$$\begin{aligned} \frac{d^2G_x^*}{dx^2} &= \frac{\partial^2 G}{\partial x^2} - \frac{\left( \frac{\partial^2 G}{\partial x \partial y} \right)^2}{\frac{\partial^2 G}{\partial y^2}} \\ &= \frac{\frac{\partial^2 G}{\partial x^2} \frac{\partial^2 G}{\partial y^2} - \left( \frac{\partial^2 G}{\partial x \partial y} \right)^2}{\frac{\partial^2 G}{\partial y^2}} = 0. \end{aligned} \quad (\text{A9})$$

This condition is equivalent to Eq. (A2). Similarly, we can prove the equivalence by using the variable  $y$ :

$$\begin{aligned} \frac{d^2G_y^*}{dy^2} &= \frac{\partial^2 G}{\partial y^2} - \frac{\left( \frac{\partial^2 G}{\partial x \partial y} \right)^2}{\frac{\partial^2 G}{\partial x^2}} \\ &= \frac{\frac{\partial^2 G}{\partial x^2} \frac{\partial^2 G}{\partial y^2} - \left( \frac{\partial^2 G}{\partial x \partial y} \right)^2}{\frac{\partial^2 G}{\partial x^2}} = 0. \end{aligned} \quad (\text{A10})$$

### Appendix B: Derivation of the liquid droplet case

The free energy  $G$  for the case of the liquid droplet surface has the following form:

$$G(y) = \gamma S_1(y) + \gamma S_2(y) - \Delta P V_0 y, \quad (\text{B1})$$

where  $y = V_2/V_0 - 1/2$  and  $S_i(y)$  can be obtained from Eqs. (8) and (9). Minimizing  $G(y)$  with respect to  $y$ , we obtain,

$$\Delta P(y, a, \eta) = \frac{3\gamma}{R_0} \left( \frac{dS_1/S_0}{dy} + \frac{dS_2/S_0}{dy} \right). \quad (\text{B2})$$

By taking the same strategy as the fluid membrane case, the analytical expression of  $\Delta P_c$  is given as

$$\Delta P_c \approx \frac{16\sqrt{6}\gamma\varepsilon_a^{3/2}}{9R_0}. \quad (\text{B3})$$

- 
- [1] Lee, J. S.; Jen, J. F. Polymersomes for drug delivery: Design, formation and characterization. *J. Control Release* **2012**, *161*, 473-483.
- [2] Rideau, E. et al. Liposomes and polymersomes: a comparative review towards cell mimicking. *Chem. Soc. Rev.* **2018**, *47*, 8572-8610.
- [3] Discher, B. M. et al. Polymersomes: Tough Vesicles Made from Diblock Copolymers. *Science* **1999**, *284*, 1143.
- [4] Discher, D. E.; Eisenberg, A. Polymer Vesicles. *Science* **2002**, *297*, 967.
- [5] Pegoraro, C. et al. Translocation of flexible polymersomes across holes at the nanoscale. *Biomater. Sci.* **2014**, *2*, 680.
- [6] Guo, X.; Szoka, F. C. Chemical Approaches to Triggerable Lipid Vesicles for Drug and Gene Delivery. *Acc. Chem. Res.* **2003**, *36*, 335.
- [7] Joseph, A. et al. Chemotactic synthetic vesicles: Design and applications in blood-brain barrier crossing. *Sci. Adv.* **2017**, *3*, e1700362.
- [8] Zhang, Z. F.; Xu, J.; Drapaca C. Particle squeezing in narrow confinements. *Microfluid Nanofluidics* **2018**, *22*, 120.
- [9] Plaks, V.; Koopman, C. D.; Werb, Z. Circulating tumor cells. *Science* **2013**, *341*, 1186.
- [10] Zhang, Z.; Xu, J.; Hong, B.; Chen, X. The effects of 3D channel geometry on CTC passing pressure - towards deformability-based cancer cell separation. *Lab. Chip.* **2014**, *14*, 2576.
- [11] Paul, C. D.; Mistriotisvq, P.; Konstantopoulos, K. Cancer cell motility: lessons from migration in confined spaces. *Nat. Rev. Cancer* **2017**, *17*, 131.
- [12] Vormittag, P.; Gunn, R.; Ghorashian S.; Veraitch, F. S. A guide to manufacturing CAR T cell therapies. *Curr. Opin. Biotechnol.* **2018**, *53*, 164.
- [13] Gompper, G.; Kroll, D. M. Driven transport of fluid vesicles through narrow holes. *Phys. Rev. E* **1995**, *52*, 4198.
- [14] Tordeux, C.; Fournier, J.-B. Extravasation of adhering vesicles. *Europhys. Lett.* **2002**, *60*, 875.
- [15] Rangelov, B.; Milchev, A. Translocation kinetics of vesicles through narrow holes. *EPL* **2022**, *138*, 42001.
- [16] Meng, F. L.; Chen, J. Z. Y.; Doi, M.; Ou-Yang, Z.-C. Phase diagrams and interface in inflating balloon. *AIChE J.* **2014**, *60*, 1393.
- [17] Han, Y.; Lin, H.; Ding, M.; Li, R.; Shi, T. Flow-induced translocation of vesicles through a narrow hole. *Soft Matter* **2019**, *15*, 3307.
- [18] Linke, G. T.; Lipowsky, R.; Gruhn, T. Osmotically induced passage of vesicles through narrow holes. *Europhys. Lett.* **2006**, *74*, 916.
- [19] Shojaei, H. R.; Muthukumar, M. Translocation of an Incompressible Vesicle through a Pore. *J. Phys. Chem. B* **2016**, *120*, 6102.
- [20] Khunpetch, P.; Man, X. K.; Kawakatsu, T.; Doi, M. Translocation of a vesicle through a narrow hole across a membrane. *J. Chem. Phys.* **2018**, *148*, 134901.
- [21] Kantor, Y.; Kardar, M.; Nelson, D. R. Statistical Mechanics of Tethered Surfaces. *Phys. Rev. Lett.* **1986**, *57*, 791.
- [22] Doi, M. *Soft Matter Physics*; Oxford University Press, 2013.
- [23] de Gennes, P.-G.; Brochard-Wyart, F.; Quéré, D. *Capillarity and Wetting Phenomena*; Springer, 2003.